Ab initio study of charge trapping and dielectric properties of Ti-doped HfO_2

D. Muñoz Ramo,[1] A. L. Shluger,[1,2] and G. Bersuker[3]
[1]*Department of Physics and Astronomy, University College London and The London Centre for Nanotechnology, Gower Street, London WC1E 6BT, United Kingdom*
[2]*WPI Advanced Institute for Materials Research, Tohoku University, 2-1-1 Katahira, Aoba, Sendai 980-8577, Japan*
[3]*SEMATECH, 2706 Metropolis Drive, Austin, Texas 78741, USA*
(Received 14 July 2008; revised manuscript received 17 September 2008; published 8 January 2009)

The electronic structure and relative stability of monoclinic, tetragonal, and cubic phases of HfO_2 with Ti doping in the range of 3.125%–37.5% are studied by means of first-principles calculations. The dielectric response, and electron and hole trapping properties of Ti-doped monoclinic HfO_2 are calculated using a hybrid density-functional B3LYP. The incorporation of Ti into HfO_2 induces higher polarizability of Hf and O ions, accompanied by an increase in the static dielectric constant and softening of phonon modes. However, the Ti ions serve as deep electron traps inducing localized levels in the gap and, at high Ti concentrations, the HfO_2 conduction-band offset with Si is effectively reduced by about 1.5 eV.

DOI: 10.1103/PhysRevB.79.035306 PACS number(s): 61.72.Bb, 61.72.J−, 71.20.−b, 77.84.Bw

I. INTRODUCTION

The continuous hunt for higher transistor densities per unit chip area while minimizing power consumption drives the semiconductor industry to employ new materials with higher dielectric constants κ (the so-called high-k dielectrics) than that in the conventional SiO_2 based transistors. Higher values of κ permit reducing the equivalent oxide thickness (EOT) of the dielectric layer while preserving acceptable gate leakage current. For this application, the dielectric has to satisfy a set of rather strict criteria including a sufficiently high band offset with respect to the Si substrate, thermal stability, low concentration of electrically active defects, and minimum intermixing with the metal electrode materials and SiO_2 ultrathin film (usually used as an interfacial layer with the Si substrate). Currently, only Hf-based dielectrics provide acceptable trade offs with respect to these mutually contradicting requirements although the κ value of HfO_2 in its most stable monoclinic form does not exceed 24.[1–3] However, continuous device scaling calls for gate dielectric stacks with even higher κ to improve electrostatic control over the transistor channel while keeping the parasitic gate leakage current at a sufficiently low level. Therefore, some kind of modification to the HfO_2 structure/composition which would increase its κ value without compromising the above mentioned device characteristics is highly desirable.

In this respect, research is being conducted into possibilities of increasing κ through doping different phases of HfO_2. There are no general rules and two different ways have been tried so far. One is through stabilization of phases of HfO_2, which exhibit larger values of κ than the low-temperature monoclinic (m)-HfO_2 but are unstable at room temperature in the undoped form. For example, doping of HfO_2 with Si,[4,5] Al,[6] and Y (Refs. 7 and 8) stabilizes the tetragonal phase of HfO_2 at room temperature, with κ values of the order of 70. However, in many cases the concentration of oxygen vacancies dramatically increases due to the aliovalent character of the dopant cation, which may have a detrimental effect on the performance of metal-oxide-semiconductor field-effect transistors (MOSFETs).[6–8] Another approach is to mix HfO_2 with higher κ materials, such as TiO_2 (κ=80–110 at room temperature[9]). An increase in the value of κ up to 90% has been reported in some Ti-doped high-κ gate stacks.[10,11] It is unclear whether this increase is related to TiO_2 segregation in the HfO_2 matrix, or to changes in the electronic structure of HfO_2 induced by the presence of Ti dopant ions. However, the use of Ti or other ions as dopants may impact on other gate stack characteristics, such as leakage current and charge trapping in the dielectric. In this respect, Paskaleva *et al.*[12] have reported new electron trapping processes in MOSFETs using Ti-doped Hf silicates with a characteristic trapping energy of about 0.9 eV. The exact nature of the state responsible for these processes still has not yet been elucidated.

Several theoretical calculations using a periodic model and the density functional theory (DFT) within the local density approximation (LDA) or the generalized gradient approximation (GGA) have been performed to investigate the mechanisms determining the value of κ in different phases of m-HfO_2 and in other compounds.[3,13,14] In particular, Dutta *et al.*[15] have reported an increase in the value of κ in Ti-doped ZrO_2 with homogeneous distribution of Ti in Zr sites and a reduction in the band gap of the system. Cockayne[16] has reported similar trends in HfO_2 doped with several impurities, among them Ti. Recently, Lee *et al.*[17] carried out density-functional calculations of relative stabilities of monoclinic, tetragonal, and cubic phases of HfO_2 doped with several cation dopants and predicted that at high concentrations dopants such as Ti, with ionic radii smaller than Hf, should stabilize the tetragonal phase but destabilize the cubic phase.

However, in these LDA/GGA calculations the band gap of the system is significantly underestimated, which may affect the accuracy of prediction of the value of κ and of the band-gap reduction. In addition, LDA favors delocalization of electrons in the system, making it less suitable than some other methods for studying charge trapping processes in these materials. More sophisticated methods, which predict band gaps in better agreement with experiment, have been used to study charged oxygen vacancies[18–20] as well as the electron and hole self-trappings in perfect m-HfO_2.[21] Using

any of these methods to study the dielectric constant modification in Ti-doped HfO_2 phases as well as related charge trapping properties could be beneficial for more comprehensive understanding of these systems and developing better understanding of the mechanisms of dielectric constant engineering.

In this work, we used DFT with a hybrid density functional and both periodic and embedded-cluster models to investigate the mechanisms that control the dielectric constant change, and to study the electronic structure and electron/hole trapping properties of m-HfO_2 doped with 3.125%–37.5% of Ti ions. The paper is organized as follows. In Sec. II we describe the details of the models and methods used for our electronic structure calculations. The electronic structure of Ti-doped HfO_2 is described in Sec. III. The results concerning the dielectric properties of different phases of Ti-doped HfO_2 are presented in Sec. IV. In Sec. V we examine the electron and hole trappings in the system. Finally, our conclusions are presented in Sec. VI.

II. COMPUTATIONAL DETAILS

To study the electronic structure, phonon spectrum, and dielectric properties of Ti-doped m-HfO_2, we used a periodic model and the CRYSTAL06 package.[22] This method makes use of local basis sets of Gaussian-type orbitals (GTOs) and consistently demonstrates good performance in studying the electronic structure of a broad class of insulators.[23,24] We employ an all-electron basis set on oxygen ions, which has been used previously to study a wide range of oxides,[25,26] with the outer exponents optimized for better description of m-HfO_2.[20] It includes 14s, 6p, and 1d functions contracted to 1s and 3sp shells using a 8/411/1 scheme. For Hf atoms we used a small relativistic effective core potential (RECP) introduced by Stevens *et al.*[27] and adapted for the CRYSTAL code.[20] 12 outer electrons are considered explicitly while the core electrons and the nucleus are substituted by an effective core pseudopotential. The basis set consists of 6s, 6p, and 4d functions contracted to 3sp and 2d shells using a 411/31 scheme. For Ti, we used a Lanl2 RECP substituting all but 12e in the atom,[28] and a basis set optimized for the rutile phase of TiO_2 consisting of 6s, 6p, and 5d functions contracted to 3sp and 3d shells using a 411/311 scheme. These basis sets are thoroughly described on the CRYSTAL website.[29]

We used different supercell sizes depending on the amount of doping considered. A 96-atom $2\times2\times2$ supercell was used for calculations involving the undoped phase and the 3.125%-doped phase. This doping concentration corresponds to substituting one of the Hf atoms in a supercell by Ti. A Monkhorst-Pack mesh of nine k points in the irreducible part of the Brillouin zone was used for the integration in the reciprocal space. A smaller 24 atom $1\times1\times2$ supercell was used for higher amounts of doping due to larger computational costs involved. Three amounts of Ti doping: 12.5, 25, and 37.5 % mol (one, two, and three Hf atoms substituted by Ti, respectively), were studied using 36 k points.

Both atomic coordinates and cell parameters were optimized in the 24-atom supercell while for the 96-atom supercell only atomic coordinates were optimized and lattice parameters were taken from a calculation performed on undoped m-HfO_2.[20] A convergence tolerance of 10^{-10} a.u. for the total energy was used in the self-consistent-field (SCF) calculations involving both geometry optimization and dielectric constant calculations. The geometry optimization was performed for each supercell with the tolerances set to 0.0005 a.u. Å^{-1}, 0.0003 a.u. Å^{-1}, 0.002 Å, and 0.001 Å for the maximum gradient, average gradient, maximum displacement, and average displacement, respectively. A uniform charge background was applied in the charge trapping calculations to compensate the extra charge of the supercell.

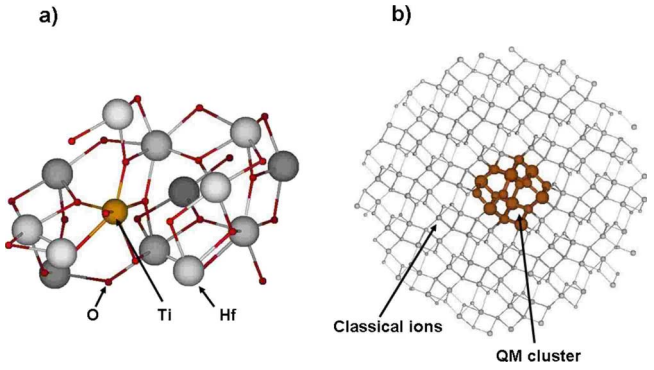

FIG. 1. (Color online) Schematics of the embedded-cluster model used in this work. (a) QM cluster; (b) detail of the classical region surrounding the QM cluster.

Most of the calculations were performed using the hybrid B3LYP exchange-correlation functional.[30,31] There is a general consensus that this functional gives good description of the structure and other properties of simple and magnetic oxides, along with their surfaces,[23,24,32–34] perovskites,[24] m-HfO_2,[20,21] and other wide band-gap materials.[35] It has also been used successfully to model the electron and hole trappings in HfO_2,[21] crystalline and amorphous SiO_2,[36,37] and inorganic electrides.[38]

To investigate the effect of the basis set and density functional in calculations of the effect of Ti doping on stability of different phases of HfO_2, and to compare with the predictions of Ref. 17, we have also carried out plane-wave GGA calculations using the Perdew-Burke-Ernzerhof (PBE) functional[39] and the projector-augmented wave method[40] in the supercells mentioned previously, using the same k-point grid as in the CRYSTAL calculations and an energy cutoff of 600 eV for the plane-wave basis set. These calculations were performed with the VASP package.[41]

To calculate the electron spin resonance (ESR) properties of trapped holes and electrons in the system, we used an embedded-cluster model described in detail in Refs. 20 and 42. This model has been used successfully to calculate the optical properties and ESR parameters of oxygen vacancies and electron and hole polarons in m-HfO_2.[20,21] Similarly to the previous work,[20,21] a quantum-mechanical (QM) cluster including the Ti substitutional defect, the distorted region accommodating the trapped hole or electron, and its vicinity (shown in Fig. 1) was embedded into the rest of the crystal represented by a lattice of classical rigid ions. We used a 96-atom unit cell of m-HfO_2, with zero charge and dipole

TABLE I. Lattice parameters (in angstroms and degrees) and unit-cell volume (in Å^3) for the cubic, tetragonal, and monoclinic phases of Ti-doped HfO_2 at different doping levels. The c parameter in the Ti-doped phases was obtained by dividing the c parameter of the supercell by two. The same operation was performed to obtain the a and b parameters in the undoped and 3.125%-doped phases. The three values for the cubic phase at 37.5% doping correspond to the fully optimized structure, which has the orthorhombic symmetry.

Phase	Parameter	0%/3.125%	12.5%	25%	37.5%
Monoclinic	a	5.151	5.123	5.113	5.045
	b	5.211	5.165	5.060	5.010
	c	5.313	5.315	5.355	5.378
	α	90.00	90.47	90.91	90.21
	β	99.48	99.31	97.37	96.37
	γ	90.00	90.31	92.10	91.27
	Volume	140.68	138.79	137.28	135.05
Cubic	a	5.081	5.051	5.023	4.978/5.127/5.081
	Volume	131.17	128.86	126.73	129.68
Tetragonal	a	5.076	5.069	5.036	4.988
	c	5.195	5.185	5.202	5.253
	Volume	133.85	133.23	131.93	130.70

moment, as a building block for constructing an approximately spherical nanocluster with monoclinic symmetry containing 2016 classical ions and having a radius of about 25 Å. The coordinates of ions in this unit cell were optimized in the periodic DFT calculations using the CRYSTAL code. Then one Hf atom in the center of the nanocluster was substituted by Ti and the local geometry was modified to exactly match the lattice relaxation induced by the trapped charge as obtained in the periodic CRYSTAL calculations up to a certain radius. This radius was chosen to be about 5 Å as the displacements of ions induced by the charge process beyond this distance calculated in the periodic model are negligibly small. This computational scheme is implemented in the GUESS computer code,[42] which employs the GAUSSIAN package[43] for calculating the electronic structure of the QM cluster in the electrostatic potential of the rest of the lattice.

The QM cluster surrounding the Ti ion included 13 hafnium ions and 28 oxygen ions (see Fig. 1). All Hf ions outside the quantum cluster and within the radius of 10 Å from the center were represented by large-core Hay and Wadt RECPs,[28] which substitute all but four electrons of a hafnium atom. This prevents an artificial polarization of the electron density toward positive point ions outside the quantum cluster. The point ions outside the quantum cluster carry formal charges and contribute to the electrostatic potential on the quantum cluster ions (see Refs. 42, 44, and 45 for more detail). The GTO basis sets on oxygen, hafnium, and titanium ions, and the pseudopotential on Hf and Ti ions in embedded-cluster calculations are the same as in the periodic calculations. We also used the same B3LYP density functional to calculate the electronic structure and the g tensor for the trapped electron and hole.

III. PROPERTIES OF TI-DOPED HFO_2

A. Structure and phase separation

The Ti substitution in m-HfO_2 induces changes in the local lattice structure of the system. In the relatively dilute 3.125% concentration case, the Ti ion is displaced by 0.2 Å into an off-center position away from the Hf site. As a result, the Ti-O distances to the two threefold coordinated ($3C$) oxygen ions reduce by 0.2 Å while those to the two fourfold coordinated ($4C$) oxygen ions increase by 0.3 Å. Other Ti-O distances remain mostly unaffected. The displacements of ions in the next coordination shell are less than 0.1 Å, and those beyond 4 Å from Ti are negligible.

The geometry relaxation around the Ti ion obtained in the 3.125%-doped phase is also present at higher amounts of doping and is accompanied by the reduction in the lattice parameters with increasing doping level. The b and β parameters gradually decrease, with a difference between the undoped cell and the 37.5%-doped cell of about 4% and 1%, respectively. The volume of the cell decreases by about 4% as doping increases to 37.5%, as shown in Table I.

To explore the possibility that other phases of HfO_2 are stabilized by the introduction of Ti in the lattice, we calculated the energies of optimized supercells of cubic and tetragonal Ti-doped HfO_2 with the same distribution of Ti in the lattice as in the monoclinic supercells using both the PBE and B3LYP functionals and VASP and CRYSTAL06 codes, correspondingly. Similar to the monoclinic phase, the volume of the unit cell is reduced with increasing amount of doping. The 37.5%-doped cubic phase represents, however, a marked exception. In this case, the fully optimized structure becomes orthorhombic (see Table I), and the oxygen ions near the Ti ions adopt a three-coordinated geometric configuration. These structural features are similar to those observed in the lattice of $ZrTiO_4$.[46]

The obtained energy differences between the cubic and tetragonal phases and the monoclinic phase, ΔE_{cubic} and ΔE_{tetra}, are compared with the energy differences found for undoped HfO_2 in Table II. The results obtained with two methods are qualitatively similar. In all cases, the monoclinic phase is the most stable one. ΔE_{tetra} is smaller in the 3.125% and 12.5% phases than in the undoped one, and becomes

TABLE II. Energy per formula unit of the cubic and tetragonal phases with respect to the monoclinic phase, and formation energy for Ti-doped m-HfO_2 with different amounts of doping. All energies are shown in eV/molecule.

Doping level	ΔE_{tetra} (PBE)	ΔE_{tetra} (B3LYP)	ΔE_{cubic} (PBE)	ΔE_{cubic} (B3LYP)	E_{form}
0%	0.18	0.12	0.30	0.16	
3.125%	0.17	0.09	0.27	0.11	0.001
12.5%	0.15	0.08	0.38	0.26	0.002
25%	0.15	0.22	0.46	0.39	0.06
37.5%	0.20	0.22	0.07	0.04	0.06

larger at higher amounts of doping. ΔE_{cubic} increases with increasing amount of doping up to 25% and shows a trend for destabilizing the cubic phase, in agreement with predictions by of Lee *et al.*[17] ΔE_{cubic} drops significantly at 37.5% doping if a full optimization of the supercell is performed in accordance with the greater stability of the orthorhombic titanate phase at this high concentration. If, however, the cubic symmetry is constrained through the optimization process, ΔE_{cubic} becomes 0.55 eV in PBE keeping the trend of increasing destabilization of the cubic phase.

We also analyzed the differences in total energies arising from different dopant distributions in the supercells. The energies of configurations where Ti ions are close are by 0.1 eV per molecule higher than those where Ti ions are on average more separated from each other. For our study we chose the lowest energy cells, corresponding to the disperse Ti distribution. We also evaluated the possibility of phase separation by calculating the formation energy E_{form} as the difference between the energy per molecule of the doped phases and the sum of energies per molecule of pure m-HfO_2 and TiO_2 in the rutile phase (see Table I). In all cases the value of E_{form} was less than 0.1 eV per molecule, suggesting a subtle balance of the enthalpy and configuration entropy contribution to the free energy.

We estimated the configuration entropy contributions as $S_{conf}=3.6\times10^{-5}$ eV/K per formula unit for the 25%-doped phase and $S_{conf}=4.3\times10^{-5}$ eV/K per formula unit for the 37.5%-doped phase. Thus the solid solution at thermal equilibrium can only be stabilized at high temperatures, which are of the order of 1670 K for the 25%-doped phase and 1380 K for the 37.5%-doped phase. This result suggests that phase segregation of TiO_2 particles in the matrix of HfO_2 could contribute to the large dielectric constant increase observed in doped HfO_2 thin layers.[10,11] The results for relatively homogeneous distribution of Ti, presented below, demonstrate only about 30% increase in the dielectric constant.

B. Electronic structure

The electronic structure of m-HfO_2 is modified by incorporation of Ti. At 3.125% doping, Ti d states produce a twofold-degenerate state just below the conduction-band minimum (CBM) and a threefold degenerate state between 1.0 and 1.5 eV below the CBM (see Fig. 2). The Ti-induced bands split and become wider as the Ti concentration increases (see Fig. 2), and transform into two broad Ti bands effectively reducing the band gap. The position of the valence-band maximum (VBM) is largely unaffected by the presence of Ti in the lattice; therefore one can estimate the conduction-band offset with Si as about 1.5 eV in the 25%- and 37.5%-doped supercells. This band offset reduction is in qualitative agreement with the recent calculations by Cockayne[16] but our calculations predict an offset reduction by 0.4 eV larger than that obtained in Ref. 16 by the LDA method.

According to Mulliken population analysis, effective Ti charges (+2.4e) are reduced with respect to Hf (+2.8e) in all cells, indicating that Ti is in fact negatively charged with respect to the lattice. Oxygen charges depend on the coordination number and proximity to Ti. As in the perfect crystal, charges on 4C oxygen are on average −1.4e and, on 3C oxygen ions, −1.3e. However, 3C oxygen connected to Ti ions have reduced charges of −1.2e, effectively shielding its negative charge.

IV. DIELECTRIC CONSTANT CALCULATION

The static dielectric constants for Ti-doped monoclinic phase are computed using the relation:

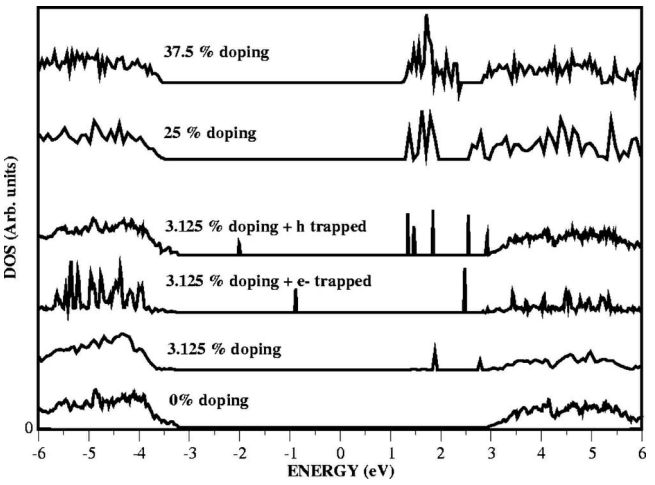

FIG. 2. Total density of states of m-HfO_2 at different levels of Ti doping, in neutral cell, and with electron or hole trapped.

TABLE III. Average Born effective charges, and diagonal elements of κ for pure and Ti-doped m-HfO_2 with different amounts of doping.

	Z^*_{Hf}	Z^*_{Ti}	Z^*_{O3C}	Z^*_{O4C}	κ_{xx}	κ_{yy}	κ_{zz}
0% Ti	5.06		−2.56	−2.51	19.07	17.54	14.45
25% Ti	5.22	5.14	−2.62	−2.58	21.68	22.07	19.52
37.5% Ti	5.33	5.24	−2.66	−2.53	24.03	23.88	19.54

$$\kappa_{\alpha\beta} = \kappa^{\infty}_{\alpha\beta} + \frac{4\pi}{M_0 V}\sum_{\lambda}\frac{\hat{Z}^*_{\lambda\alpha}\hat{Z}^*_{\lambda\beta}}{\omega^2_{\lambda}}, \quad (1)$$

where $\kappa^{\infty}_{\alpha\beta}$ is the high-frequency dielectric tensor, M_0 is a reference mass (1 in our case), V is the volume of the supercell, ω_λ is the frequency of phonon λ, and $\hat{Z}^*_{\lambda\alpha}$ is the mode effective charge calculated as

$$\hat{Z}^*_{\lambda\alpha} = \sum_{i\beta} Z^*_{i,\alpha,\beta}(M_0/M_i)^{1/2}\epsilon_{i,\lambda,\beta},$$

with M_i being the mass of ion i, $Z^*_{i,\alpha,\beta}$ being the Born effective charge tensor component corresponding to ion i, and $\epsilon_{i,\lambda\beta}$ being the eigendisplacement of ion i in the phonon mode λ. The Born effective charges relate polarization of the ions with their displacements in the lattice. Assuming that $\kappa^{\infty}_{\alpha\beta}$ is mainly unaffected by the presence of Ti, one can use an isotropic value of 5.0 for all phases.[3]

Born effective charge tensors calculated for the ions of the undoped phase show small anisotropy with diagonal components, being one order of magnitude larger than off-diagonal components. The average values of Z^* for each type of ion at different levels of doping are shown in Table III. In general, the values obtained with the B3LYP functional for the undoped phase are about 0.1–0.2 units smaller than those obtained with the LDA method.[3,13,16] One can see that Ti doping results in increased Z^* for all ions in the cell and especially for the Hf ions. The value of Z^* for Ti ions is larger than the value for Hf in the undoped phase but it is slightly smaller than the value for Hf in the doped phases.

The increase in the values of Z^* may be attributed to the changes in electronic structure induced by the presence of Ti in the lattice. The magnitude of Z^* is related to changes in hybridization of the oxygen occupied p bands and the cation unoccupied d bands when ions are displaced in oxides;[47] these changes, which can be related to the transfer of charge between cation and anion during ion displacement, are linked to the energy difference between the oxygen p and cation d bands (corresponding to the band gap in this particular case), as has been observed in *ab initio* calculations performed on several perovskites.[47,48] Thus, the difference between the values of Z^* in the undoped phase calculated with B3LYP and the values obtained with the LDA functional may be related to the different values of the band gap obtained with these two functionals; the larger gap obtained in B3LYP results in the reduction in the Z^* values compared with those obtained with LDA. For the same reason, the reduction in the band gap of HfO_2 induced by the incorporation of Ti d levels should promote the increase in the values of Z^* in the material. Increased anisotropy of the system with increasing amount of Ti doping should also contribute to larger values of Z^*.[47]

The phonon density of states at the Γ point calculated with the B3LYP functional for the perfect and doped m-HfO_2 are shown in Fig. 3 (a Gaussian smearing factor of 0.2 cm^{-1} was used to construct this diagram). Values for the undoped phase are close to those obtained with the GGA or LDA functionals.[3,13] The incorporation of Ti induces a spread of phonon modes around the values found in the perfect structure and creation of the new modes in the low-frequency part of the spectrum, below 100 cm^{-1}.

The diagonal elements of the static dielectric constant obtained at different doping levels are shown in Table III. The static dielectric constant increases with the amount of Ti doping by the factor of 1.24 at 25% doping and by the factor of 1.32 at 37.5% doping. The Ti doping also slightly increases the anisotropy of the dielectric tensor. The average values of κ for the undoped and 25%-doped phases are slightly larger than those calculated using the LDA functional (κ=16.5 and 19.5, respectively).[3,13,16]

The contributions of phonon modes to the trace of κ at different doping levels are presented in Fig. 4. One can see that in the perfect m-HfO_2 the main contributions come from the few phonon modes in the 200–400 cm^{-1} region while in the doped phase the contributions are distributed among a larger number of modes starting from lower frequencies. The largest contributions to κ come from phonon modes involving mainly displacements of O ion in the lattice. These contributions are enhanced in the Ti-doped crystals due to several factors. The higher ion polarizabilities and the smaller

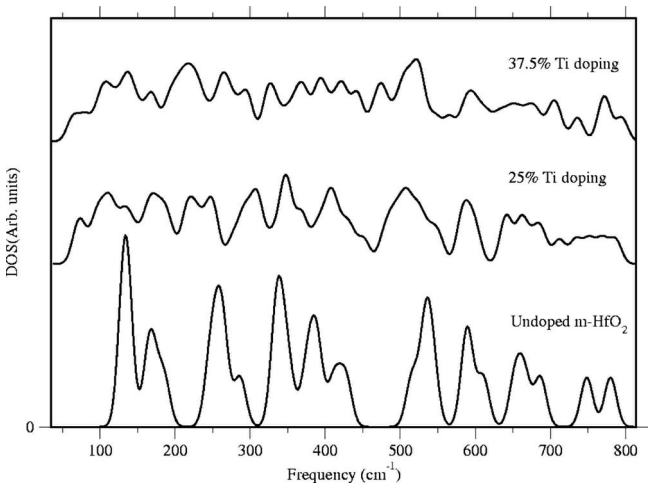

FIG. 3. Phonon density of states at the Γ point for three phases of m-HfO_2 with different amounts of doping.

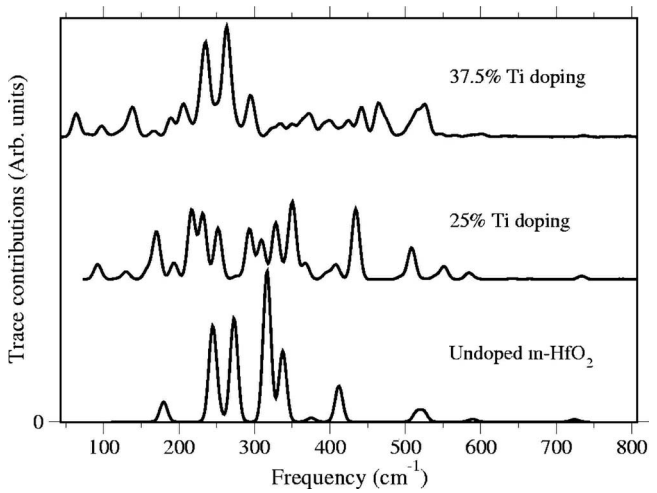

FIG. 4. Relative contributions of the phonon modes at the Γ point to the trace of κ for three phases of m-HfO_2 with different amount of Ti doping.

symmetry of the cell allow more modes to have nonvanishing contributions. The region of the phonon spectrum where the active phonons are located is shifted toward lower frequencies with increasing doping content. The reduction in cell volume increases the value of the dielectric tensor but this contribution is relatively small. In order to establish which contribution (Born charges or phonons) is more important to explain the increase in κ, we compared its value for the undoped phase with the value obtained from the calculation of κ in this phase, substituting the values of Born charges by the values obtained for the 25% doped phase. We also substituted the mass of one of the Hf atoms by the mass of Ti. The resulting value of κ is only 4% larger than the original value. This suggests that the main contribution to the increase in κ originates from the changes in the phonon spectrum induced by the presence of Ti.

V. ELECTRON AND HOLE TRAPPING

We have recently predicted[21] that electron polarons can be localized on up to three Hf ions, and that hole polarons can be localized at $3C$ and $4C$ oxygen ions in the perfect m-HfO_2 lattice. Ti doping induces additional trapping sites in the m-HfO_2 lattice with corresponding changes in the electronic structure and spin distribution of the system. The stability of these trapping states can be estimated by means of the calculation of their trapping energies with respect to electron (hole) states that are far from impurity. The trapping energy is defined as the difference between the total energies of the fully relaxed trapped state in the lattice and the delocalized electron (hole) in the conduction (valence) band of undoped perfect HfO_2 in the following way (conserving the number of electrons):

$$E_{\text{trap}} = (E_{\text{dop},q} + E_{\text{perf}}) - (E_{\text{dop}} + E_{\text{perf},q}), \quad (2)$$

where E_{trap} is the trapping energy of the state considered. The first bracket corresponds to the state of the system where the electron or hole is trapped on a defect in a fully relaxed state,

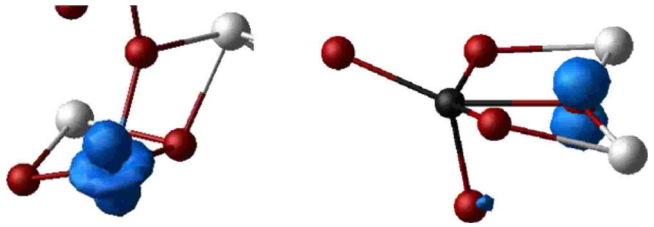

FIG. 5. (Color online) Spin density (S=0.057) of trapped electron (left) and trapped hole (right) states in Ti-doped HfO_2 (3.125% doping level).

where $E_{\text{dop},q}$ is the total energy of the supercell corresponding to the hole (electron) trapped in the Ti-doped HfO_2, and E_{perf} corresponds to the total energy of the supercell describing the neutral undoped m-HfO_2. The second bracket corresponds to the state where the electron or hole are delocalized in a perfect lattice far from the impurity, where E_{dop} is the energy of the neutral Ti-doped HfO_2 supercell, and $E_{\text{perf},q}$ corresponds to the total energy of the supercell describing the electron (hole) delocalized in the conduction (valence) band of perfect undoped m-HfO_2. In this approximation, we neglect the effect of impurities on free electron or hole states and $E_{\text{perf},q}$ is calculated by including a hole or electron in the perfect cell of HfO_2. In the case of the electron, the extra charge becomes evenly spread over all Hf ions while in the case of the hole, it is delocalized by all oxygen ions. No localized level is created in the gap. This ensures that this solution is a good representation of the charge carrier being at the bottom of the conduction band/top of the valence band far from the impurity.

Our calculations suggest that in a relatively dilute 3.125%-doped phase Ti ions serve as deep electron traps with almost no spin-density spread to the nearby ions, as shown in Fig. 5. This distribution is very different from that found for the electron polaron in the undoped lattice, which shows electron localization on three nearby Hf ions.[21] The relaxation of the lattice is restricted mainly to a radius of 3 Å around the Ti ion. This ion is displaced away from the $3C$ oxygen sublattice and is now located near the ideal position of the undoped m-HfO_2 cation sublattice, producing an elongation of the Ti-O($3C$) bonds and a reduction in the Ti-O($4C$) bonds with respect to the neutral situation. The electron trapping energy on Ti ion is −2.82 eV, which is much larger than the trapping energy of −0.32 eV of electron polaron in the undoped lattice. The electronic state of the trapped electron is located about 3.6 eV below the CBM (see Fig. 2), which is about 3.1 eV lower than the localized state induced in the case of the undoped lattice. This large energy gain with respect to the unoccupied state is caused by the larger electron affinity of the Ti ion than that of Hf ion, and by the stronger lattice polarization induced by the fully localized extra electron.

To model electron trapping at a higher doping level of 25%, we duplicated the 24-atom supercell used previously for this phase in the X and Y directions to generate a 96-atom supercell and added an extra electron into the system. As in the 3.125% case, the electron is trapped upon just one Ti ion in the lattice and induces similar distortions in the local ge-

TABLE IV. Principal values of the g tensor for trapped electron and hole in Ti-doped HfO_2 (3.125% doping level). Values for self-trapping in undoped HfO_2, calculated in Ref. 21, are also shown for comparison.

State	g_1	g_2	g_3
Hole	2.012	2.021	2.045
Electron	1.958	1.970	1.987
Hole (undoped)	2.014	2.025	2.040
Electron (undoped)	1.812	1.829	1.922

ometry around the trapping center. The electron trapping energy is smaller, of the order of −2.3 eV, reflecting the higher kinetic energy of an extra electron in the broader Ti impurity band (see Fig. 2).

Our calculations for the 3.125%-doped phase demonstrate that holes can trap on 3*C* O ions neighboring Ti in a polaron state similar to that in perfect *m*-HfO_2.[21] As in the perfect lattice case, the lattice relaxation induced by this state is short ranged, showing only large displacements in the nearest-neighbor cations. These ions displace by about 0.1 Å away from the oxygen ion bearing the hole.

The hole spin density is localized mainly at one 3*C* oxygen ion, with small contributions from the nearest-neighbor oxygen (see Fig. 5). This distribution is similar to that found for the hole 3*C* polaron in the undoped lattice. The hole trapping energy for this state is about −0.06 eV. This is much smaller than the hole polaron trapping energy of −0.57 eV in the perfect *m*-HfO_2 and demonstrates how a smaller, isovalent impurity can destabilize hole trapping. We note that hole trapping to compensate aliovalent impurities and cation vacancies is well known in oxides,[49] with only some examples of isovalent impurity hole traps (e.g., Ge in SiO_2).

The hole one-electron level is split by about 1.0 eV from the VBM (see Fig. 2); a similar value is found for the hole polaron in undoped *m*-HfO_2. We were unable to obtain a stable hole localized at a 4*C* oxygen ion near Ti.

Using the embedded-cluster model, we calculated the principal values of the g tensor for the trapped hole and electron in order to provide guidance for experimental detection of these states. The results are shown in Table IV, which also show values for the electron and hole polarons calculated previously.[21] The g-tensor value for the trapped hole has orthorhombic symmetry although the differences between components are small. This value is similar to that obtained for the hole trapped in the undoped phase due to the similar nature of the localized state in both cases. The value obtained for the trapped electron is, in comparison, smaller and more anisotropic. It is also very different from the value obtained for the trapped electron in the undoped material, in agreement with the fact that it is now localized on Ti ion.

VI. CONCLUSIONS

In conclusion, our calculations predict that doping with Ti will lead to destabilization of the cubic phase of HfO_2. The components of the static dielectric tensor in Ti-doped *m*-HfO_2 at homogeneous distribution of impurity should increase with Ti concentration by about 30%. This increase in κ is caused primarily by higher polarizabilities of the Hf and O ions in the presence of Ti ions, as well as softer active phonons and lower symmetry of the unit cell with respect to the undoped phase. We also observed that the conduction-band offset with silicon is reduced by about 1.5 eV at large Ti-doping concentrations due to formation of a Ti band. Besides, the Ti ions may act as deep electron traps and contribute to fixed charge formation. Thus incorporation of Ti ions into the Hf-based dielectrics can lead to EOT reduction (assuming that associated technological difficulties can be overcome) and help to meet the gate stack scaling requirements although this may come at the price of reduced reliability of devices.

ACKNOWLEDGMENTS

This work was funded by the EPSRC-GB Grant No. GR/S80080/01 and the Grant-in-Aid for Creative Scientific Research (Grant No. 16GS0205) from the Japanese Ministry of Education, Culture, Sports, Science, and Technology. Computer time on the HPCx facility was awarded to the Materials Chemistry Consortium under EPSRC-GB Grant No. GR/S13422/01 "Materials Chemistry using Teraflop Computing". We are grateful to J. Gavartin and K. P. McKenna for valuable comments. D.M.R. would like to thank K. Hermansson and her research group for their hospitality and financial support during his stay at Uppsala University.

[1] K. Kukli, J. Ihanus, M. Ritala, and M. Leskela, Appl. Phys. Lett. **68**, 3737 (1996).
[2] E. P. Gusev, E. Cartier, D. A. Buchanan, M. Gribelyuk, M. Copel, H. Okorn-Schmidt, and C. D'Emic, Microelectron. Eng. **59**, 341 (2001).
[3] G.-M. Rignanese, J. Phys.: Condens. Matter **17**, R357 (2005).
[4] K. Tomida, K. Kita, and A. Toriumi, Appl. Phys. Lett. **89**, 142902 (2006).
[5] T. S. Böscke, S. Govindarajan, P. D. Kirsch, P. Y. Hung, C. Krug, and B. H. Lee, Appl. Phys. Lett. **91**, 072902 (2007).
[6] P. K. Park and S.-W. Kang, Appl. Phys. Lett. **89**, 192905 (2006).
[7] K. Kita, K. Kyuno, and A. Toriumi, Appl. Phys. Lett. **86**, 102906 (2005).
[8] T. S. Böscke *et al.*, Tech. Dig. - Int. Electron Devices Meet. **2006**, 255.
[9] G. D. Wilk, R. M. Wallace, and J. M. Anthony, J. Appl. Phys. **89**, 5243 (2001).
[10] Q. Fang *et al.*, Thin Solid Films **428**, 263 (2003).
[11] D. H. Triyoso, R. I. Hedge, X.-D. Wang, M. W. Stoker, R. Rai, M. E. Ramon, B. E. White, and P. J. Tobin, J. Electrochem. Soc.

153, G834 (2006).
[12] A. Paskaleva, A. J. Bauer, M. Lemberger, and S. Zürcher, J. Appl. Phys. **95**, 5583 (2004).
[13] X. Zhao and D. Vanderbilt, Phys. Rev. B **65**, 233106 (2002).
[14] P. Broqvist and A. Pasquarello, Appl. Phys. Lett. **90**, 082907 (2007).
[15] G. Dutta, K. P. S. S. Hembram, G. Mohan Rao, and U. Waghmare, J. Appl. Phys. **103**, 016102 (2008).
[16] E. Cockayne, J. Appl. Phys. **103**, 084103 (2008).
[17] C.-K. Lee, E. Cho, H.-S. Lee, C. S. Hwang, and S. Han, Phys. Rev. B **78**, 012102 (2008).
[18] J. Robertson, Rep. Prog. Phys. **69**, 327 (2006).
[19] P. Broqvist and A. Pasquarello, Appl. Phys. Lett. **89**, 262904 (2006).
[20] D. Muñoz Ramo, J. L. Gavartin, A. L. Shluger, and G. Bersuker, Phys. Rev. B **75**, 205336 (2007).
[21] D. Muñoz Ramo, A. L. Shluger, J. L. Gavartin, and G. Bersuker, Phys. Rev. Lett. **99**, 155504 (2007).
[22] R. Dovesi, V. Saunders, C. Roetti, R. Orlando, C. M. Zicovich-Wilson, F. Pascale, B. Civalleri, K. Doll, N. M. Harrison, I. J. Bush *et al.*, *CRYSTAL06 User's Manual* (University of Torino, Torino, Italy, 2006).
[23] R. Dovesi, B. Civalleri, R. Orlando, C. Roetti, and V. R. Saunders, Rev. Comput. Chem. **21**, 1 (2005).
[24] F. Cora, M. Alfredsson, G. Mallia, D. S. Middlemiss, W. C. Mackrodt, R. Dovesi, and R. Orlando, Struct. Bonding (Berlin) **113**, 171 (2004).
[25] M. D. Towler, N. L. Allan, N. M. Harrison, V. R. Saunders, W. C. Mackrodt, and E. Apra, Phys. Rev. B **50**, 5041 (1994).
[26] F. Cora, Mol. Phys. **103**, 2483 (2005).
[27] W. J. Stevens, M. Krauss, H. Basch, and P. G. Jasien, Can. J. Chem. **70**, 612 (1992).
[28] P. J. Hay and W. R. Wadt, J. Chem. Phys. **82**, 270 (1985).
[29] http://www.crystal.unito.it/Basis_Sets/Ptable.html.
[30] A. D. Becke, J. Chem. Phys. **98**, 5648 (1993).
[31] C. Lee, W. Yang, and R. G. Parr, Phys. Rev. B **37**, 785 (1988).
[32] A. Wander, I. J. Bush, and N. M. Harrison, Phys. Rev. B **68**, 233405 (2003).
[33] A. Wander and N. M. Harrison, Surf. Sci. **457**, L342 (2000).
[34] J. R. B. Gomes, I. D. R. Moreira, P. Reinhardt, A. Wander, B. G. Searle, N. M. Harrison, and F. Illas, Chem. Phys. Lett. **341**, 412 (2001).
[35] J. Muscat, A. Wander, and N. M. Harrison, Chem. Phys. Lett. **342**, 397 (2001).
[36] A. V. Kimmel, P. V. Sushko, and A. L. Shluger, J. Non-Cryst. Solids **353**, 599 (2007).
[37] L. Giordano, P. V. Sushko, G. Pacchioni, and A. L. Shluger, Phys. Rev. Lett. **99**, 136801 (2007).
[38] P. V. Sushko, A. L. Shluger, M. Hirano, and H. Hosono, J. Am. Chem. Soc. **129**, 942 (2007).
[39] J. P. Perdew, K. Burke, and M. Ernzerhof, Phys. Rev. Lett. **77**, 3865 (1996).
[40] P. E. Blöchl, Phys. Rev. B **50**, 17953 (1994).
[41] G. Kresse and J. Hafner, Phys. Rev. B **47**, 558 (1993).
[42] P. V. Sushko, A. L. Shluger, and C. R. A. Catlow, Surf. Sci. **450**, 153 (2000).
[43] M. J. Frisch *et al.*, *GAUSSIAN 03 Revision C02* (Gaussian Inc., Wallingford, CT, 2003).
[44] J. Carrasco, C. Sousa, F. Illas, P. V. Sushko, and A. L. Shluger, J. Chem. Phys. **125**, 074710 (2006).
[45] D. Muñoz Ramo, P. V. Sushko, and A. L. Shluger, Phys. Rev. B (to be published).
[46] R. E. Newnham, J. Am. Ceram. Soc. **50**, 216 (1967).
[47] P. Ghosez, J.-P. Michenaud, and X. Gonze, Phys. Rev. B **58**, 6224 (1998).
[48] A. Filippetti and N. A. Spaldin, Phys. Rev. B **68**, 045111 (2003).
[49] O. F. Schirmer, J. Phys.: Condens. Matter **18**, R667 (2006).